Author manuscript, published in "Journal of Physical Chemistry C 116 (2012) 15117-15125"
DOI : 10.1021/jp303414c

hal-00719432, version 1 - 19 Jul 2012

Nanostructured Non-adhesive Surfaces for Micro- and Nanomanipulation

Jérôme Dejeu,[a] Mikhael Bechelany,*[b] Elise Berodier,[c] Patrick Rougeot,[a] Johann Michler[b] and Michaël Gauthier[a]*

[a] FEMTO-ST Institute, AS2M Department, UMR CNRS 6174-UFC/ENSMM/UTBM, 24 rue Alain Savary, 25000 Besançon, France

[b] European Institute of Membranes (IEM ENSCM UM2 CNRS UMR 5635), University of Montpellier 2, Place Eugene Bataillon, 34095 Montpellier, France

[c] Materials Science & Technology, Laboratory for Mechanics of Materials and Nanostructures, Feuerwerkerstrasse 39, CH-3602 Thun, Switzerland

jerome.dejeu@univ-fcomte.fr, Mikhael.Bechelany@univ-montp2.fr, elise.berodier@gmail.com, patrick.rougeot@femto-st.fr, johann.michler@empa.ch, michael.gauthier@femto-st.fr,

RECEIVED DATE (to be automatically inserted after your manuscript is accepted if required according to the journal that you are submitting your paper to)

Dr. Mikhael Bechelany, Phone: +33467149167, Fax: +33467149119, Mikhael.Bechelany@univ-montp2.fr

ABSTRACT. Adhesion between microgripper end-effector and a nano/micro-object is a main topic for manipulation in micro- and nanoscale. Tuning this force is a great challenge. Adhesion force is directly

linked to the chemical composition and the surface roughness of both, the object and the gripper. Recently, we proposed a multispheres Van der Waals force model able to predict this force. The surface used was structured by an array of polystyrene spheres with radii from 35 nm to 2 µm. The experimental pull-off forces have confirmed our model. In this present work, we analyzed other innovating structure such as non-closed packed polystyrene (PS) spheres and organized Si Nanostructures, formed by chemical etching. The adhesion values of the pull-off force measured on these structures were very low (in the range of 2 to 10 nN), and suggest that these new structures have non-adhesive properties. A new model taking in account the roughness and the organization of the PS spheres and Si Nanostructures has been developed to predict these new properties.

INTRODUCTION

hal-00719432, version 1 - 19 Jul 2012

The assembly and micromanipulation of nano/micro-components is a major issue. Manufactured products are getting smaller while they combine more and more utilities. The major issue lies in the drastic reliance of the micro/nano-objects behavior and the surface forces.[1] The manipulation of these objects involves the handling, positioning, and releasing while avoiding any disturbances of the surface forces such as capillary, van der Waals, or electrostatic forces.[2] Several application fields are concerned such as telecommunications, bioengineering, or usually all Micro-Electro-Mechanical Systems (MEMS). In the microworld, surface forces are non-negligible compared to volume forces (weight, buoyancy, etc.). Microhandling methods are mostly based on two general approaches which consist in exploiting the surface forces[3-5] (e.g. capillary grippers) or reducing the surface forces (e.g. reducing adhesion on tweezers). This paper deals with the second challenge and especially on the reduction of adhesion between tweezers and the grasped object.. One approach to reduce the adhesion force has been developed in liquid and dry medium by surface structuring[1,6-8] or chemical functionalization.[9-13] Surface nanostructuring is able to reduce the contact area between the gripper and the objects, and therefore decreases the contact area and van der Waals forces. Two approaches allow the surface structuring: top-down[14, 15] and bottom-up approaches[16, 17]. There are also methods based on the combination of both approaches.[18,19] Among these methods, the nanospheres lithography [20] has received great consideration as a result of its simplicity compare to conventional lithography techniques. Using this methods, patterning of a wide variety of solid substrates has been achieved including metals,[21-24] semiconductors,[25-27] and ceramics.[28]

Recently, we reported the influence of the structuring surface by closed-packed polystyrene (PS) spheres on the adhesion forces. We proposed a multispheres van der Waals force model which may suggest the existence of an optimal value of the sphere radius that would minimize the adhesion.[8] This model has been extended to demonstrate the existence of a minimum independent of the diameter and the nature of the spheres.[1] In this paper, and in order to understand the influence of organization, nature of nanostructures and roughness on adhesion properties, measurement has been performed on non-organized Nanowires (NWs), non-closed packed array of PS spheres and organized Si NWs produced by

hal-00719432, version 1 - 19 Jul 2012

metal induced chemical etching. The measurement shows that these new structures have non-adhesive properties. A new model has been developed to predict the adhesion force between a rough non-closed packed and a microsphere. The pull-off forces predict by the model are compared to experimental data and are concordance.

EXPERIMENTAL SECTION

Materials

Commercially available PS microspheres suspension (d ≈ 900 nm, 2.53 wt% aqueous dispersion, and d ≈ 200 nm, 2.53 wt% aqueous dispersion) was used (Polysciences, Inc., Eppelheim, Germany) as received. Acetone, toluene, hydrofluoric acid (HF, 48 %), Ammonium hydroxide (NH_4OH,25 %), Sulfuric acid (H_2SO_4, 98 %), sodium dodecyl sulfate (≥ 99.0 %), Nitric acid (HNO_3, 70 %) , Hydrochloric acid (HCl, 37 %)and Hydrogen peroxide (H_2O_2, 30 %), were purchased from Aldrich. p-type Si wafers (> 10 Ω .cm), (100) crystal orientation from Silicon Materials, USA.

Synthesis of non-organized and non-structured NWs

P-type Si wafers were used as substrates. Prior to patterning, the Si specimens were pre-cleaned in acetone to remove the organic contaminants, and were then heated in air at 600 °C for 10 min to increase the thickness of the oxide layer. The substrate was then treated with a 1:1:5 solution of NH_4OH (25 %), H_2O_2 (30 %), and water at 80 °C for 15 min to obtain a hydrophilic Si surface.[23] Hydrophilic surfaces were formed by the terminal silanol (SiOH) groups. After this pre-treatment, a monodisperse suspension of PS microspheres was spin coated onto the substrate. The suspension was dried in air at Room Temperature (RT), and the spheres arranged themselves into a closed-packed structure of two-dimensional ordered lattices due to attractive capillary forces. In order to fabricate an Au thin film pattern, the dense packed PS spheres are used as a shadow mask. Thin Au films were deposited onto the Si substrate through the PS honeycomb shadow mask using a Balzers SCD 040 sputter coater at a discharge current of 25 mA in a vacuum with pressure below 1 Pa for the desired time. After sputtering,

hal-00719432, version 1 - 19 Jul 2012

the PS mask was removed by immersing the specimens in 97 % toluene in an ultrasonic bath. Finally, the specimens were annealed at 1000 °C for 1 h (heating rate 10 °C min^{-1}) under vacuum and then cooled down to RT.

Structured surfaces: Organized non-closed pack of PS spheres

The two dimensional (2D) PS sphere ordered lattices were achieved by self-assembly using commercially available PS spheres suspension of 900 nm and 200 nm of diameter onto silicon substrate. In a standard procedure, Si wafers were cut into 1.5 cm² pieces and were pre-cleaned in acetone for 5 min and in 1 wt% HF for 5 min to remove both organic contaminants and the native oxide. Additionally, the specimens were immersed in H_2O_2/H_2SO_4 solution for 10 min and afterwards treated by O_2 plasma to produce a hydrophilic surface. After this pre-treatment, a monodisperse suspension of 10 µL of PS spheres was released onto the substrate. Then the sample was immersed into deionized water. Two droplets of sodium dodecyl sulfate solution (10 %) were deposited onto the water surface and the sample was removed out of the water, holding tilted in order to remove PS spheres in excess to the PS monolayer. After the complete drying of the substrate, the spheres were reduced by Reactive Ion Etching process (RIE) in order to obtain a non-closed packed array of spheres. The spheres were finally stuck on Si substrate by a thermal treatment at 100 °C for 30 min.

Structured surfaces: Organized non-closed pack of Si NSs

A non-closed packed array of spheres was prepared as mentioned before. A thin Au film was deposited then by sputtering. The sputtering was carried out at a discharge of 25 mA in a vacuum with the pressure below 0.1 mbar. By this Physical Vapor Deposition (PVD) step a mask of Au was obtained and the thickness of this layer was measured around 400 nm between spheres.[27] The specimens covered by Au were etched in a solution of HF/H_2O_2 (4 M/0.88 M) in water at room temperature. After removing the metal with aqua regia (HNO_3/HCl in a volume ratio of 1:3) solution and immersing the sample into toluene at 50 °C to dissolve the PS spheres, Si samples were dried and fully characterized.

hal-00719432, version 1 - 19 Jul 2012

hal-00719432, version 1 - 19 Jul 2012

Characterization

Samples were characterized by Scanning Electron Microscopy (SEM, Hitachi S-4800), and energy dispersive X-ray spectroscopy (EDX, Genesis 4000 EDAX).

Force Distance Measurement by Atomic Force Microscopy

Characterization of the pull-off force was performed with a commercial atomic force microscope (AFM; stand-alone SMENA scanning probe microscope NT-MDT, Russian). The experiments were done under a controlled environment with a laminar flow (humidity 30 % and 25 °C) on the Nanorol platform (http://nanorol.cnrs.fr/events.php). The rectangular silicon AFM cantilever, whose stiffness is 0.3 N/m, was fixed, and the substrate moved vertically. The same kind of cantilever was used for all experiments. As the objective of this work is to improve the reliability of micro-object manipulation, interactions have been studied between a micrometric sphere and a structured surface. Measurements were in fact performed with a cantilever where a sphere (radius r_1) was glued in place of the standard AFM tip. In order to measure interaction forces in an experimental comparable to micromanipulation framework, the radius $r_1$of the sphere glued on the AFM is 5µm. The force calibration was performed for each cantilever with its resonance frequency, and 10 measurements were done at different locations on the same sample with a driving speed of 200 nm/s.

RESULTS

Synthesis methods and Morphologies

Non-organized NWs. In order to understand the influence of organization of Si NWs on their adhesion properties, non-organized NWs has been synthesized as reported elsewhere.[23] SEM characterizations show the formation of a forest of NWs (Figure 1). EDX characterization shows that these NWs are composed of oxidized silicon.

Non-closed pack of PS spheres. From one closed-packed PS sphere arrays on substrate, several non-closed-packed arrays were produced by reducing the initial sphere diameter with RIE process (Figure 2). 900 nm diameters were shrunk to 800 nm, 710 nm, 560 nm, 495 nm for respectively 1 min, 2 min, 5 min and 7 min of RIE process (Figure 2a-e).

Non-closed packed of organized Si nanostructures. Non-organized Si nanostructures has been synthesized as reported elsewhere.[24] Figure 3 shows the regular pattern of Si NWs synthesized by selective metal inducing chemical etching process. The advantage of this method as compared to other lithographic methods is that it is simple and fast. In addition, both diameter and density of PS sphere can be controlled to a certain extent, so that pattern variations can be easily achieved. By modifying the size of the PS spheres, the dimension of the Si NWs and their spatial density can be changed.[24] Figure 3 shows Si NWs arrays resulting from the use of PS spheres with diameters of 200 nm, and 900 nm respectively. The diameter of the resulting Si NWs is 70 nm (Figure 3a) and 400 nm (Figure 3b) and the spatial density is ~2.89 x 10^9 cm^{-2} (Figure 3a) and ~1.43 x 10^8 cm^{-2} (Figure 3b-d), respectively. By decreasing the size of the PS spheres used in the beginning, we decrease the dimension of the Si NWs and increase their density. We note here that it is also possible to tune the diameter of the NWs by conserving the same spatial density using different conditions of RIE as well as the length using different immersing times during metal assisted chemical etching (Figure 3c,d). EDX measurement shows the presence only of oxygen and silicon in the specimens.

Adhesion measurement

Organized and non-organized Si NWs. The pull-off force was measured by AFM for different silica types: wafer, non-organized and organized NWs. The adhesion curves were presented in Figure 4. The pull-off force was influenced by the texture of the silica (wafer or nanowire). The adhesion force is lower on surface with nanowires than on silica wafer. The reason is the decrease of the contact surface. On the non-organized nanowires curve (Figure 4a), the release between the probe and the surface is

hal-00719432, version 1 - 19 Jul 2012

hal-00719432, version 1 - 19 Jul 2012

performed step by step and the curve presents discontinuous jumps. This phenomenon is already observed in the case of adhesion force measurement on carbon and boron nitride nanotubes.[29-31] The previous measurements are summarized and compared with silicon surface in Table 1.

The adhesion force with silica layer as homogeneous or NWs decreasing the pull-off compares to silicon surface which is near 250 nN. The surface with organized nanowires has a pull-off force inferior to the other silica materials. The Si NWs values of the pull-off force are very weak close to the detection limit of the AFM. Consequently the comparison between the different sizes of Si NWs cannot be done due to the lack of accuracy for this range of values. However the low pull-off forces from NWs surface confirm that nanostructure decreases greatly the adhesion forces. In addition, the diameter and the length of the Si NWs seem to have no effect on the pull-off force value.

Non-closed pack of PS spheres. It was found in a previous study on closed pack of PS spheres arrays that the sphere size influences the pull-off force. The decrease of PS spheres size reduces the adhesion force near 100 times as compare to uncoated substrate. We can expect the same behavior with the non-closed pack of PS spheres. The force measurements on the non-closed packed samples are presented in Figure 5 and are summarized in Table 2. The pull-off force, after shrinkage, is lower than that of the initial sphere. Indeed, for 900 nm diameter, the adhesion is 149 nN and decreases up to 10 nN with spheres of 495 nm of diameter.

DISCUSSION

Non-organized NWs

Compared to organized Si NWs, non-organized NWs present a different behavior in term of adhesion force. The discontinuous jumps observed in Figure 4 can be explain by two phenomena depending on the contact number between the probe and the NWs. If this number is one, i.e. just one nanowire is attaching to the probe; the discontinuous jump is explained by Ishikawa *et al.* [29]. The number of

discontinuous jumps increases with the length of the NWs. The first jumps are a mesoscale peeling. The small stick-slip behaviors are also observed at the slope, which exhibit a nanoscale intermittent peeling without sliding. After, the jump corresponds to a conformational transition of the nanowires. The following slope, with no stick-slip behaviors, is the sliding of the contact point between the nanowire and the silicon substrate or the stretching of the NW. In the work reported by Ishikawa *et al.*[29], just one slope without stick-slip has been observed. In our experiment the graph of Figure 4 shows three slopes without nanoscale intermittent peeling. This finding could be related to the fact that the probe is in contact with several NWs and the adhesion force is performed between the AFM cantilever and several NWs. In this case, the retract curve (Figure 6) is explained as previously, mesoscale intermittent peeling (B-C) then conformational transition or first broken up (C-D). These two steps are followed by nanoscale intermittent peeling (D-E) before the broken of the contact between the probe and the NWs, nanowire by nanowire. The steps from F to J, is the same that D to F with an uncertainty on the jump G-H which is either a conformational transition, or a broken link. In order to confirm exactly the phenomena, the experiments should be performed in-situ inside a SEM but the incertitude on the mechanism does not modify the conclusion on the NW using for the micromanipulation. The schema of Figure 6 resumes the different steps of the Figure 4a with no conformational transition.

Non-closed pack of PS spheres

The pull-off force measured between a sphere and a PS structured surface by AFM can be simulated by van der Waals monospheres model established by Dejeu *et al.*[1,8] because the radius of the PS sphere is superior to 100 nm. The authors modeled the pull-off force between a structured surface and a sphere whatever the nature and the size of both spheres respectively deposited on the surface and glued on the tipless cantilever extremity.[1] We suggest to modify and to expand the model in order to determine the pull-off force for a non-closed pack of PS spheres. The typical model of van der Waals force on smooth spheres is reported below (equation 1):

hal-00719432, version 1 - 19 Jul 2012

$$F_{vdw} = \frac{(A_1\ A_2)^{1/2}\ r_1\ \lambda\ r_2}{6\ z_0^2\ (r_1 + d\ r_2)} \quad (1)$$

where r_1 is the sphere radius glued on the tipless cantilever extremity, r_2 is the initial PS sphere radius respectively, λ is the PS radius sphere reduction coefficient due to the etching process, A_i the Hamaker constants of materials, z_0 the contact distance.

The simulation results and the comparison with the experimental measurements are summarized in Table 2. The simulated pull-off force is superior to the experimental measurements for all the non-closed packed PS spheres. This phenomenon can be attributed to the spheres roughness increasing after shrinkage process.

Actually whereas the polymer sphere size is reduced, oxygen plasma bombardment causes also roughness on the PS sphere surface. The roughness induced by plasma etching has been widely reported.[32] Figure 1e shows the etched PS spheres of 495 nm reduced from 900 nm. Although the initial spherical surface is smooth and clean (Figure 1a), nanoscale roughness appears on the spherical surface after the plasma etching. The roughness is more noticeable with longer etching process time. The surface roughness has been attributed to microscopically inhomogeneous etching.[33,34]

Again when the roughness increases, the contact area between the two surfaces (probe and substrate) decreases[35] and in turns this decreases the contact surface and the van der Waals forces. All studies conducted to observe the influence of roughness on the pull-off force converge to the same conclusion: the higher the roughness, the smaller the pull-off force is. [36-42] Tormoen *et al.* [38,39] reported that if the size of the asperities is of the same order of magnitude as the particle, the contact area as well as the pull-off forces decreases. The roughness plays also an important role in the error sources for the pull-off force measurements.[43] This error increases with the roughness.[38,39] In conclusion, the surface roughness would decrease the bond strength; nevertheless it would be more difficult to predict the forces since it becomes very noisy.

hal-00719432, version 1 - 19 Jul 2012

The modeling of the roughness could be done in different ways from fractal modeling to simplified geometries[1,8,44,45]. The first modeling is based on a complete definition of the roughness profile, enabling the construction of a precise model whose parameters are still difficult to identify in a practical case. The second modeling based on simplified geometry is based on assumptions on the roughness geometry but contains few parameters (or at least only one). In order to discuss the impact of roughness on the adhesion forces, we chose to simulate simulate the roughness by a simplified geometry consisting in a collection of nanospheres (radius, r_3) on the PS spheres periphery. The relative position between the probe and the spheres respectively the roughness r_3, on the sphere r_2, is described in Figure 7. As the pull-off force is a direct consequence of van der Waals force between both objects, the experimental pull-off measurements can be compared with van der Waals models. In the previous papers, we have shown that when the radius r_2 is greater than 100 nm, the pull-off force can be simulated by the interaction between the probe and only one or three spheres on the PS sphere depending on the initial position of the probe against the substrates. So four interaction cases between the probe and the PS spheres are possible (Figure 7):

_ Case 1: The probe is aligned and in contact with one asperity on one PS sphere, Figure 7a

_ Case 2: The probe is in the middle of three asperities on one PS sphere and in contact with them, Figure 7b

_ Case 3: The probe is in the middle on the three PS spheres and in contact with one asperity on each PS sphere, Figure 7c

_ Case 4: The probe is in the middle on the three PS spheres and in contact with three asperities on each PS sphere, Figure 7d.

The four total forces F between a PS sphere with roughness r_3 and the probe is described below:

$$F_{\text{case 1}} = \sum_{i,j}^{\mathbb{Z}^2} \frac{A_{12}\ r_1\ r_2}{6 z_{ij_{\min}}^2 (r_3 + r_1)} \cdot \frac{r_3 + z_0 + r_1}{r_3 + z_{ij_{\min}} + r_1} \qquad (2)$$

hal-00719432, version 1 - 19 Jul 2012

$$F_{case\,2}=\sum_{i,j}^{\mathbb{Z}^2}\frac{A_{12}\ r_1\ r_2}{6z_{ij_{max}}^2\,(r_3+r_1)}.\frac{\sqrt{\left(r_3+z_{ij_{max}}+r_1\right)^2-R_{ij}^2}}{r_3+z_{ij_{max}}+r_1} \tag{3}$$

$$F_{case\,3}=\sum_{i,j}^{\mathbb{Z}^2}\frac{A_{12}\ r_1\ r_2}{6z_{ij_{min}}^2\,(r_3+r_1)}.\frac{r_3+z_0+r_1}{r_3+z_{ij_{min}}+r_1}.\frac{\sqrt{\left(\lambda r_2+z_0+r_1\right)^2-\left(4\!/\!_3\,r_2^2\right)}}{\lambda r_2+z_0+r_1} \tag{4}$$

$$F_{case\,4}=\sum_{i,j}^{\mathbb{Z}^2}\frac{A_{12}\ r_1\ r_2}{6z_{ij_{max}}^2\,(r_3+r_1)}.\frac{\sqrt{\left(r_3+z_{ij_{max}}+r_1\right)^2-R_{ij}^2}}{r_3+z_{ij_{max}}+r_1}.\frac{\sqrt{\left(\lambda r_2+z_0+r_1\right)^2-\left(4\!/\!_3\,r_2^2\right)}}{\lambda r_2+z_0+r_1} \tag{5}$$

Where $z_{ij_{min}}$ and $z_{ij_{max}}$ are:

$$z_{ij_{min}}=\sqrt{\left(r_3+z_0+r_1+d_{ij}\right)^2+r_{ij}^2}-r_1-r_3 \tag{6}$$

$$z_{ij_{max}}=\sqrt{R_{ij}^2+\left(D_{ij}+\sqrt{\left(r_3+z_0+r_1\right)^2-\frac{4\,r_3^2}{3}}\right)^2}-r_1-r_3 \tag{7}$$

Where d_{ij} and D_{ij} are the projection of the distance between the center of the sphere (0;0) and the sphere (i;j) on the z axis and r_{ij} or R_{ij} on the plan (xOy) depending on the case. So these distances are done by:

$$d_{ij}=\lambda r_2-\sqrt{\left(\lambda r_2-r_3\right)^2-r_{ij}^2}-r_3 \tag{8}$$

$$D_{ij}=\lambda r_2-\sqrt{\left(\lambda r_2-r_3\right)^2-R_{ij}^2}-r_3-D_{00} \tag{9}$$

$$r_{ij}=2r_3\sqrt{i^2+j^2-ij} \tag{10}$$

$$R_{ij}=2r_3\sqrt{i^2+j^2-ij-j+\frac{1}{3}} \tag{11}$$

$$D_{00}=\lambda r_2-\sqrt{\left(\lambda r_2-r_3\right)^2-\frac{4r_3^2}{3}}-r_3 \tag{12}$$

hal-00719432, version 1 - 19 Jul 2012

This interaction model between a spherical probe and a rough sphere has been simulated using the Matlab Simulink software. The evolution of F as a function of the interaction case and of the etching time is drawn in Figure 8a,b respectively.

In Figure 8, the first points on the right-hand of the Figure are the pull-off force without roughness (when $r_2 = r_3$). The result deals with the determination of a minimum of the interaction force which represents an optimum of adhesion reduction in the applicative field of micromanipulation. In our experimental case, the optimum radius r_3 in order to minimize the adhesion is between 6 nm and 10 nm. This optimum is reached for radius 10 times smaller than in a case of a structured surface [1] with a force also ten times smaller. This value depends (i) on the interaction case between the probe and the asperities; (ii) on the borosilicate sphere radius glued to the cantilever (nature and size) and (iii) on the initial radius r_2 of the sphere. If the radius r_3 is lower than this optimum (10 nm), more and more spheres should be considered in the sum (eq 5), thus increasing the force.

Particular asymptotic convergences can be observed. In the right-hand part of the Figure, cases 2 and 3 are converging to the same values. In this case, the probe is in interaction with only the sphere(s) at distance z_0. In the cases 1, 2, 3 and 4, the sphere(s) number in interaction with the probe are 1, 3, 3 and 9 respectively. So the adhesion force is the same for the cases 2 and 3. In the left-hand part of the Figure case 1 and 2 and case 3 and 4 are converging to the same values respectively. In this case, the radius r_3 is lower than this optimum, and more and more spheres should be considered in the sum and the arrangement of the spheres is near to a plane surface, thus increasing the force. The sphere number on the sum is so important (more than 300 for r_3=1 nm) that the number of spheres r_3 in contact has no influence, and only the number of sphere r_2 should be taken into consideration. So the cases 1 and 3 are similar to the cases 2 and 4 respectively.

In Figure 8, the force decreases from 2 to 15 by an appropriate roughness of the PS sphere. This modeling range is in agreement with the experimental measurement, Table 2 with a decrease from 3 to 7. An important roughness is also observed on organized Si NWs. However, it is due to the chemical

hal-00719432, version 1 - 19 Jul 2012

etching process. It has been reported that metal induced chemical etching results in roughness along and on the top of Si NWs. [27,46] This roughness on the silicon NWs leads to a small pull-off force which is similar to one on the PS sphere after etching.

Potential application on micromanipulation

As all the experiments and the models have been established on micrometer spheres (r_1=5µm), the application of the structurations of the surface in micromanipulation can be directly discussed.

The multi-contact release observed in non-organized NWs is able to disturb the micromanipulation. Indeed it appears difficult to predict the distance required to release of all the contact. Despite the fact, that the adhesion is sensibly reduced, it seems consequently not applicable in micromanipulation application framework. The uncertainty on the distance required to the release is linked to the non-organization of NWs. Organized NWs or spheres could be another approach.

So, for manipulation, the two processes can be used to decrease the adhesion and improve the object release, with a preference for the Si NWs because of their best stability. Indeed, the PS spheres are deposited by spin coating and could left the surface during the micromanipulation tasks whereas the Si NWs are engraved on the silicon wafer.

CONCLUSION

In conclusion, experimental pull-off forces have been measured by AFM with a borosilicate sphere glued on the tipless cantilever, on both non-closed pack of PS spheres and organized Si NWs produced by metal induced chemical etching. The adhesion values obtained for both are very low, close to the detection limit of the AFM. Thus, the nanostructures used can be seen as non-adhesive surfaces. The adhesion of these non-closed packed materials has been compared to non-organized NWs. A new model has been developed to predict these new properties. So, for manipulation, the two processes can be used to decrease the adhesion and improve the object release, with a preference for the Si NWs because of their best stability. A wide range of applications, in the field of telecommunications, bioengineering, and

hal-00719432, version 1 - 19 Jul 2012

more generally speaking MEMS can be envisaged for these non-adhesive substrates. Experiments are in progress in order to investigate other organized and non-organized 1D nanostructures such ZnO,[25] BN,[47-49] SiC,[50] SiC@CNTs,[50] and Si_3N_4[51]

ACKNOWLEDGMENT. This work was partially supported by the EU under FAB2ASM, Contract FoF-NMP-2010-260079 (Efficient and precise 3D integration of heterogeneous microsystems from fabrication to assembly); and by the French National Agency (ANR) under NANOROL, Contract ANR-07-ROBO-0003, (Nanoanalyse for micromanipulation).

FIGURES.

hal-00719432, version 1 - 19 Jul 2012

hal-00719432, version 1 - 19 Jul 2012

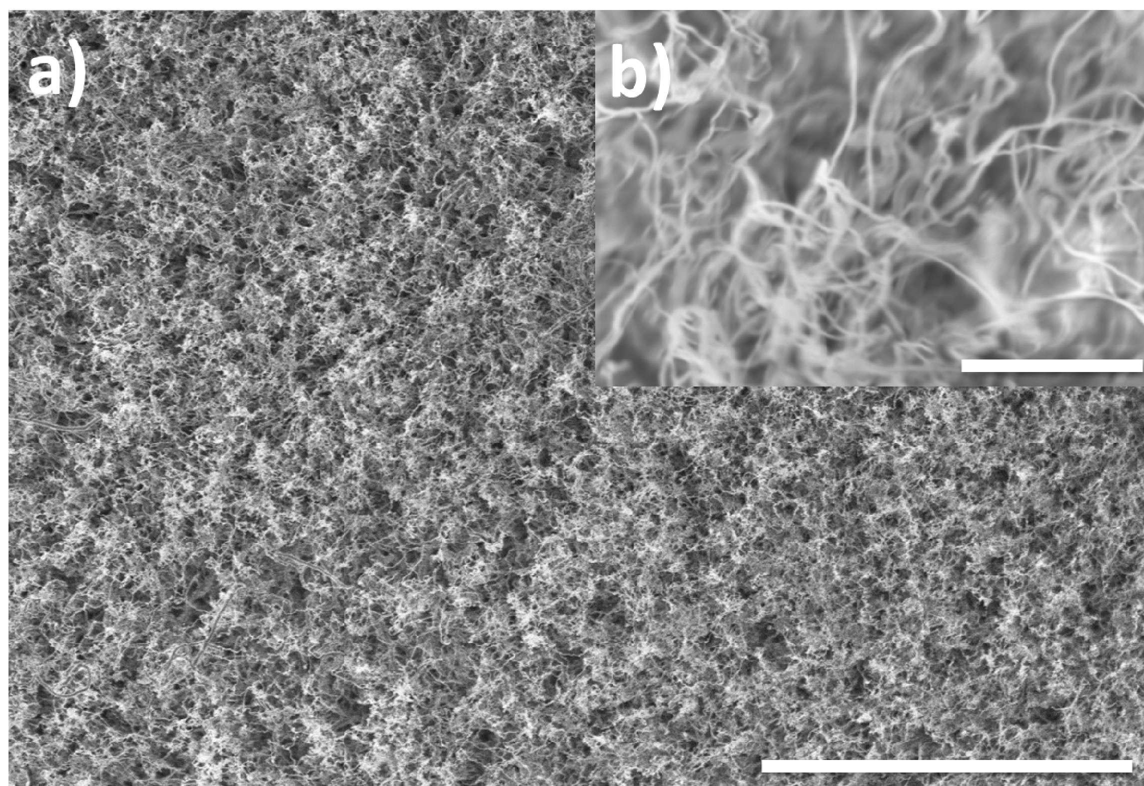

Figure 1. a) SEM image of non–organized SiO_2 NWs (scale bar = 10 μm), b) High resolution SEM image of a selected area (scale bar = 1 μm)

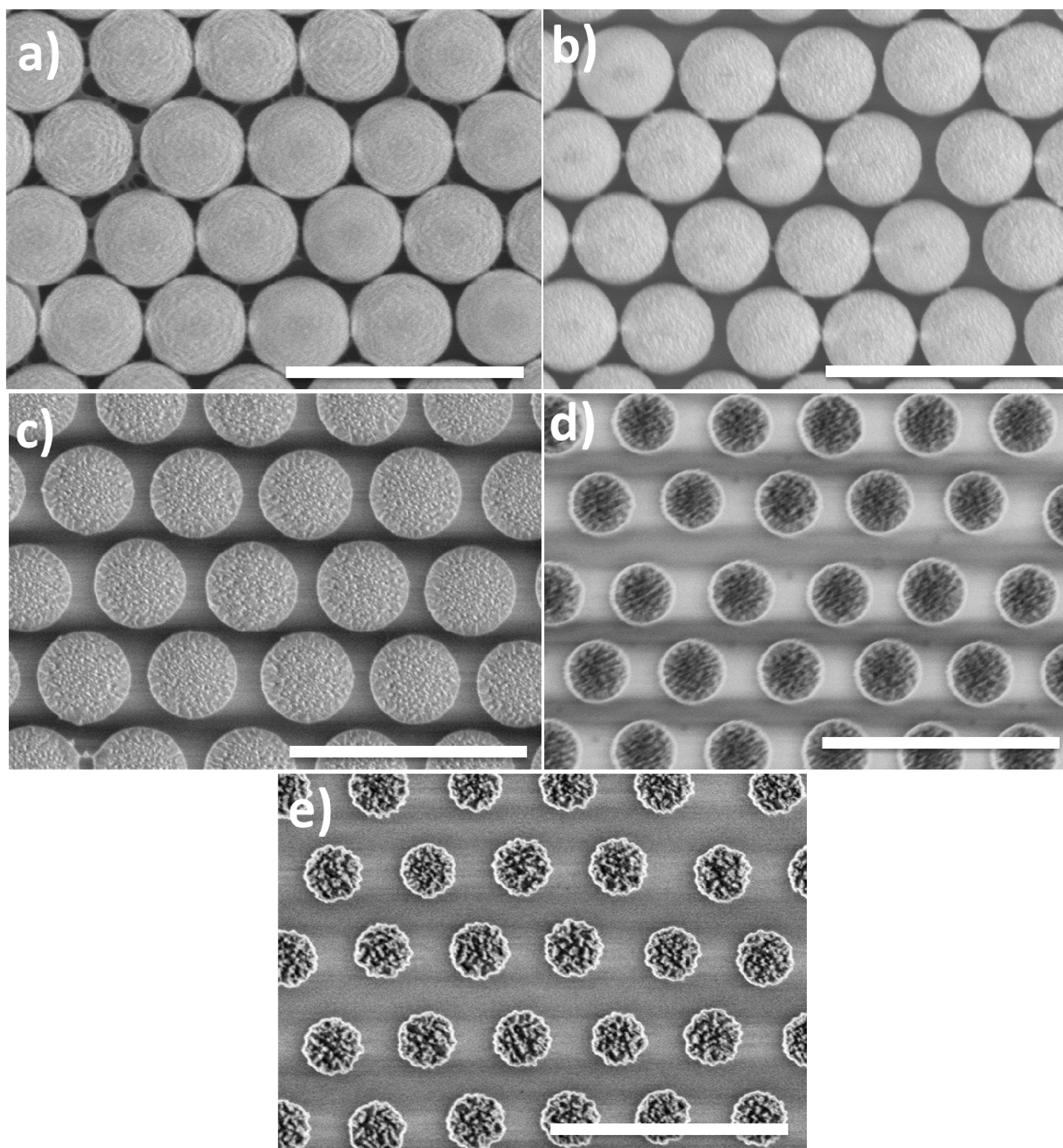

Figure 2. a) SEM images of closed-packed PS spheres arrays of 900 nm of diameter; SEM images of non-closed packed PS spheres after RIE for 1 min, 800 nm (b), 2 min, 710 nm (c), 5 min, 560 nm (d) and 7 min, 495 nm (e); (scale bars = 2 μm).

hal-00719432, version 1 - 19 Jul 2012

hal-00719432, version 1 - 19 Jul 2012

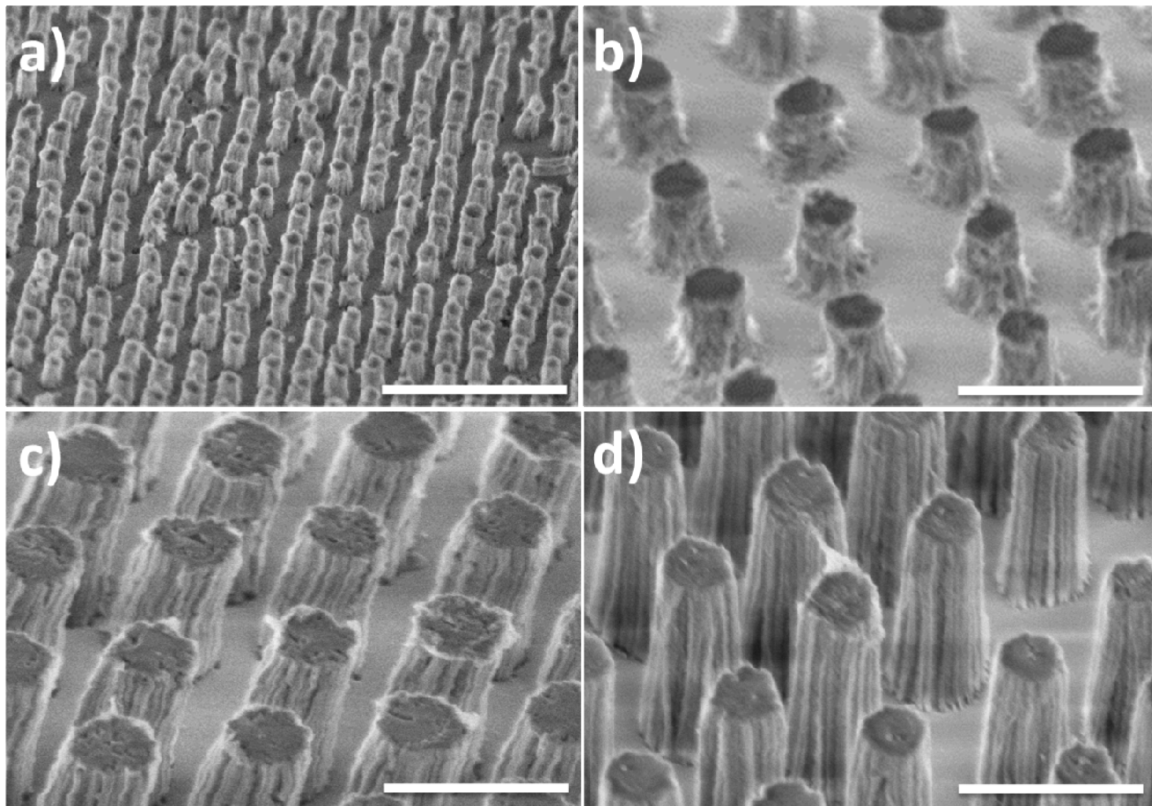

Figure.3 SEM images of different non-closed pack organized Si NWs used for the adhesion measurements synthesized used PS spheres of 200 nm (a) and 900 nm (b-c); (scale bars = 1 µm)

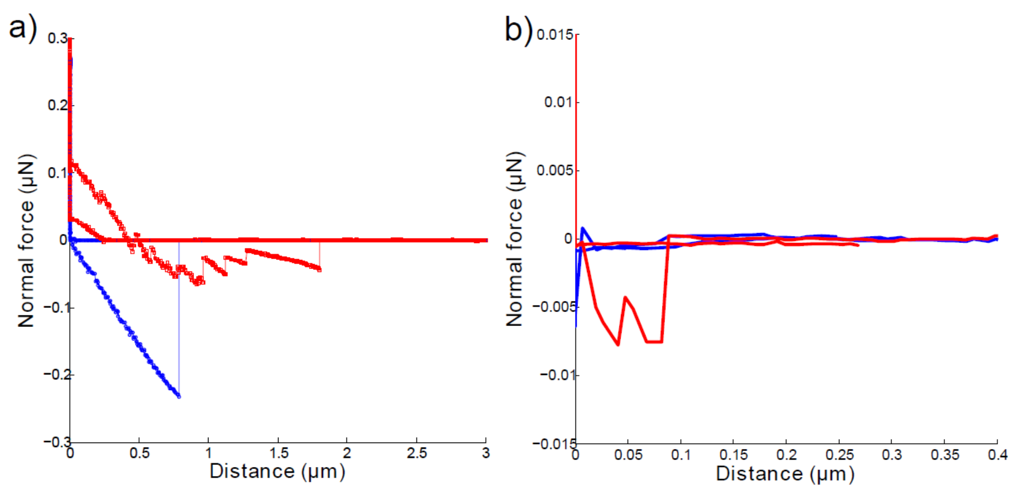

Figure 4. Adhesion force measurement: a) on silica wafer (blue curve) and non-organized nanowires (red curve) and b) on organized Si nanowires (two measurements are presented).

hal-00719432, version 1 - 19 Jul 2012

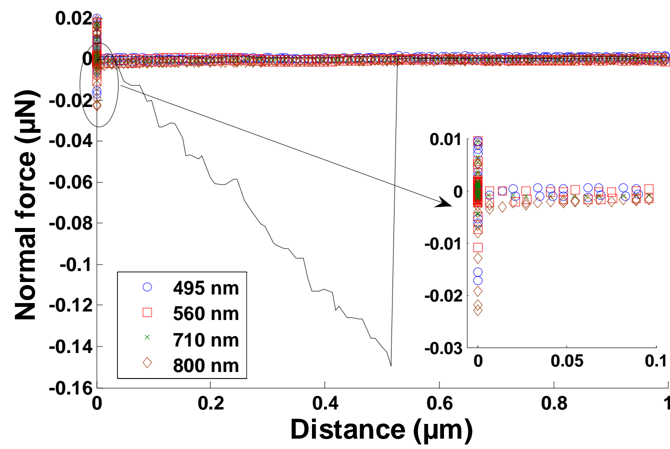

Figure 5. Pull-off force measurements on closed pack of PS spheres (900 nm, line) and non-closed pack after shrunk to 800 nm (lozenge or diamond), 710 nm (cross), 560 nm (square), 495 nm (circle).

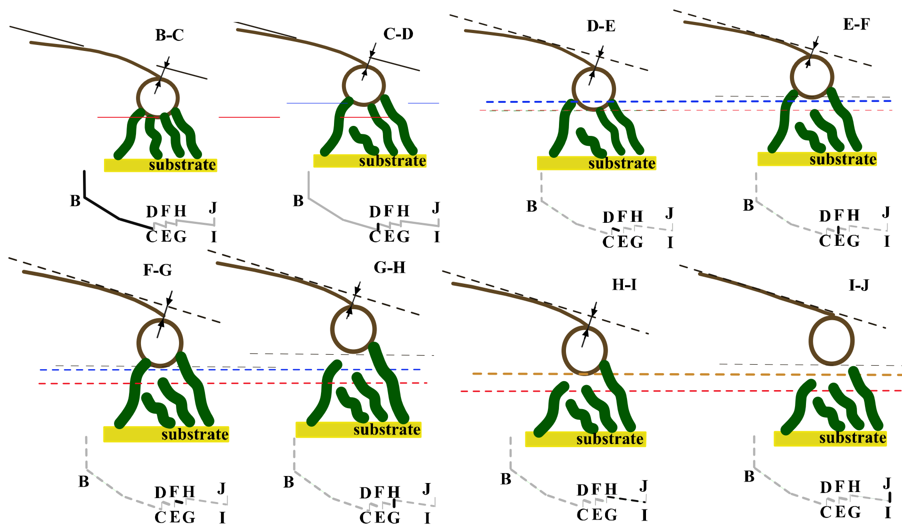

Figure 6. Schema of the adhesion between several NWs and a sphere probe with the part of the adhesion curve corresponding.

hal-00719432, version 1 - 19 Jul 2012

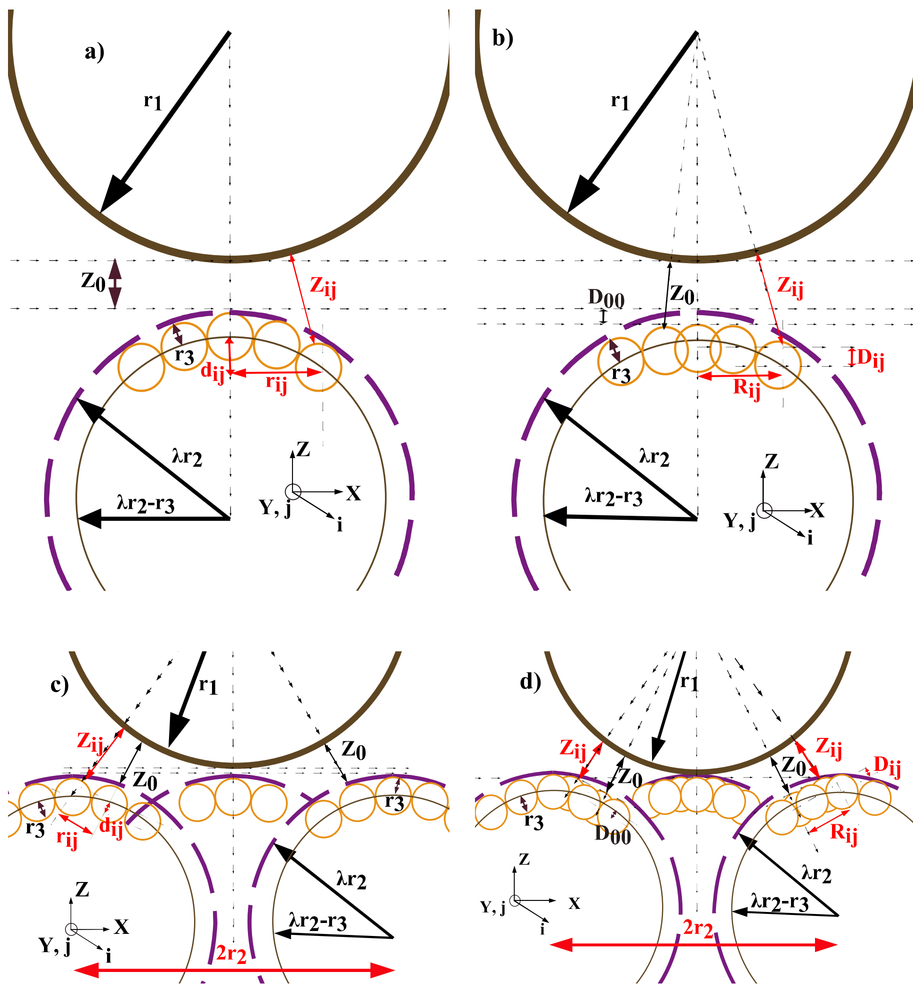

Figure 7. Description of the different interactions (a) case 1, b) case 2, c) case 3, d) case 4) between the probe r_1 and the PS spheres roughness r_3 on PS sphere r_2.

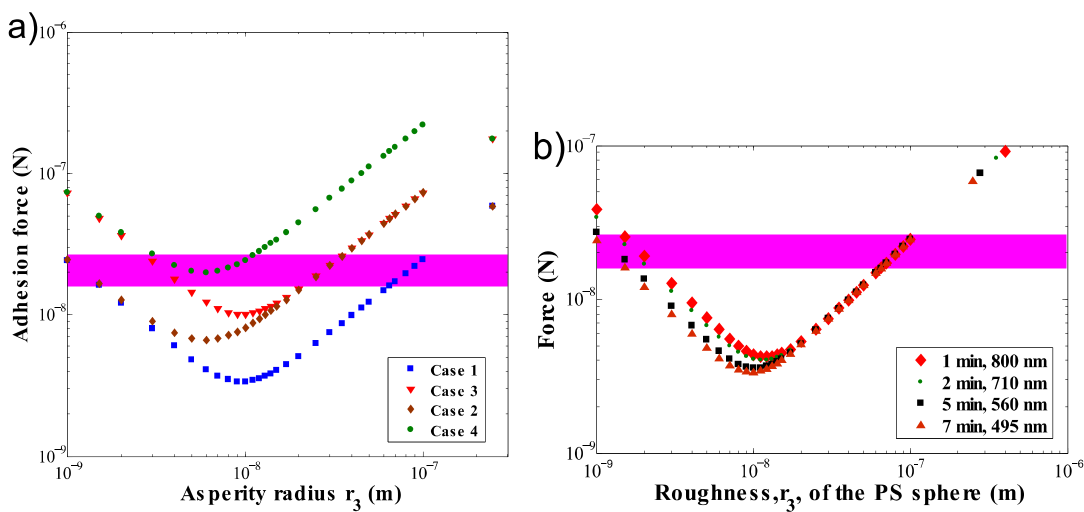

Figure 8: Theoretical pull-off forces as a function of PS sphere roughness, r_3 for the different interaction cases (a) and for the different etching time (b). The points are the theoretical values for the different cases and the pink zone are the experimental values.

hal-00719432, version 1 - 19 Jul 2012

TABLE

Table 1. Adhesion force values of different type of Si NWs arrays.

N° sample	**Sample Name**	**Spatial density [cm^{-2}]**	**Si NWs diameter [nm]**	**Si NWs lengths [nm]**	**Pull-off [nN]**
1	Si NWs	2.89×10^9	70	100	$- 3 \pm 2$
2	Si NWs	1.43×10^8	300	520	$- 7 \pm 5$

3	Si NWs	1.43 x 10^8	320	850	- 9 ± 7
4	Si NWs	1.43 x 10^8	460	1200	- 10 ± 8
5	Si wafer		-	-	- 250 ± 30

Table 2. Experimental and simulated pull-off force of nonclosed packed PS spheres.

PS spheres diameter	Experimental pull-off force (nN)	Simulated pull-off force (nN)	$F_{Pull-off_{simulated}} / F_{Pull-off_{experimental}}$
800 nm	26 ± 14	91	3.5
710 nm	12 ± 5	81	7
560 nm	10 ± 6	65	6
495 nm	13 ± 6	58	4

REFERENCES

hal-00719432, version 1 - 19 Jul 2012

hal-00719432, version 1 - 19 Jul 2012

(1) Dejeu, J.; Bechelany, M.; Rougeot, P.; Philippe, L.; Gauthier, M. *ACS Nano* **2011**, *5*, 4648.

(2) Gauthier, M.; Alo, S.; Dejeu, J.; Rougeot, P.; Reigner, S. *Submitted to IEEE TASE* **2011**.

(3) Sariola, V.; Jaaskelainen, M.; Zhou, Q. *Ieee Transactions on Robotics* **2010**, *26*, 965.

(4) Heriban, D.; Gauthier, M. *Robotic Micro-assembly of Microparts Using a Piezogripper*, 2008.

(5) Driesen, W.; Varidel, T.; Regnier, S.; Breguet, J. M. *Journal of Micromechanics and Microengineering* **2005**, *15*, S259.

(6) Li, Q.; Rudolph, V.; Peukert, W. *Powder Technology* **2006**, *161*, 248.

(7) Hodges, C. S.; Cleaver, J. A. S.; Ghadiri, M.; Jones, R.; Pollock, H. M. *Langmuir* **2002**, *18*, 5741.

(8) Dejeu, J.; Bechelany, M.; Philippe, L.; Rougeot, P.; Michler, J.; Gauthier, M. *ACS Applied Materials & Interfaces* **2010**, *2*, 1630.

(9) Dejeu, J.; Rougeot, P.; Gauthier, M.; Boireau, W. *Micro & Nano Letters* **2009**, *4*, 74.

(10) Dejeu, J.; Gauthier, M.; Rougeot, P.; Boireau, W. *ACS Applied Materials & Interfaces* **2009**, *1*, 1966.

(11) Dejeu, J.; Taouil, A. E.; Rougeot, P.; Lakard, S.; Lallemand, F.; Lakard, B. *Synthetic Metals* **2010**, *160*, 2540.

(12) Lupu, S.; Lakard, B.; Hihn, J.-Y.; Dejeu, J. r. m.; Rougeot, P.; Lallemand, S. v. *Thin Solid Films* **2011**, *519*, 7754.

(13) Lupu, S.; Lakard, B.; Hihn, J.-Y.; Dejeu, J. *Synthetic Metals* **2011**, *162*.

(14) Kim, S. H.; Kim, J.-H.; Kang, B.-K.; Uhm, H. S. *Langmuir* **2005**, *21*, 12213.

(15) Li, J.; Fu, J.; Cong, Y.; Wu, Y.; Xue, L.; Han, Y. *Applied Surface Science* **2006**, *252*, 2229.

(16) Han, J. T.; Zheng, Y.; Cho, J. H.; Xu, X.; Cho, K. *The Journal of Physical Chemistry B* **2005**, *109*, 20773.

hal-00719432, version 1 - 19 Jul 2012

(17) Hikita, M.; Tanaka, K.; Nakamura, T.; Kajiyama, T.; Takahara, A. *Langmuir* **2005**, *21*, 7299.

(18) Jiang, L.; Zhao, Y.; Zhai, J. *Angewandte Chemie International Edition* **2004**, *43*, 4338.

(19) Zhong-Ze, G.; Hong-Mei, W.; Rui-Qian, Z.; Guo-Zhi, H.; Chao, P.; Hong, Z.; Xing-Jun, T.; Zhi-Ming, C. *Artificial silver ragwort surface*; AIP, 2005; Vol. 86.

(20) Deckman, H. W.; Dunsmuir, J. H. *Natural lithography*; AIP, 1982; Vol. 41.

(21) Bechelany, M.; Brodard, P.; Elias, J.; Brioude, A.; Michler, J.; Philippe, L. *Langmuir* **2010**, *26*, 14364.

(22) Bechelany, M.; Brodard, P.; Philippe, L.; Michler, J. *Nanotechnology* **2009**, *20*, 455302.

(23) Bechelany, M.; Maeder, X.; Riesterer, J.; Hankache, J.; Lerose, D.; Christiansen, S.; Michler, J.; Philippe, L. *Crystal Growth & Design* **2010**, *10*, 587.

(24) Sakamoto, S.; Philippe, L.; Bechelany, M.; Michler, J.; Asoh, H.; Ono, S. *Nanotechnology* **2008**, *19*, 405304.

(25) Elias, J.; Lévy-Clément, C.; Bechelany, M.; Michler, J.; Wang, G.-Y.; Wang, Z.; Philippe, L. *Advanced Materials* **2010**, *22*, 1607.

(26) Lerose, D.; Bechelany, M.; Philippe, L.; Michler, J.; Christiansen, S. *Journal of Crystal Growth* **2010**, *312*, 2887.

(27) Bechelany, M.; Berodier, E.; Maeder, X.; Schmitt, S.; Michler, J.; Philippe, L. *ACS Applied Materials & Interfaces* **2011**, *3*, 3866.

(28) Yoon, T.-H.; Lee, H.-J.; Yan, J.; Kim, D.-P. *Journal of the Ceramic Society of Japan* **2006**, *114*, 473.

(29) Ishikawa, M.; Harada, R.; Sasaki, N.; Miura, K. *Physical Review B* **2009**, *80*, 193406.

(30) Whittaker, J. D.; Minot, E. D.; Tanenbaum, D. M.; McEuen, P. L.; Davis, R. C. *Nano Lett.* **2006**, *6*, 953.

(31) Hsu, J. H.; Chang, S. H. *Applied Surface Science* **2010**, *256*, 1769.

(32) Zhao, Y. P.; Drotar, J. T.; Wang, G. C.; Lu, T. M. *Physical Review Letters* **1999**, *82*, 4882.

(33) Shiu, J. Y.; Kuo, C. W.; Chen, P. L.; Mou, C. Y. *Chemistry of Materials* **2004**, *16*, 561.

(34) Haginoya, C.; Ishibashi, M.; Koike, K. *Applied Physics Letters* **1997**, *71*, 2934.

(35) Yan, L.; Wang, K.; Wu, J.; Ye, L. *Journal of Physical Chemistry B* **2006**, *110*, 11241.

(36) Heim, L. O.; Ecke, S.; Preuss, M.; Butt, H. J. *Journal of Adhesion Science and Technology* **2002**, *16*, 829.

(37) Ando, Y. *Wear* **2000**, *238*, 12.

(38) Tormoen, G. W.; Drelich, J. *Journal of Adhesion Science and Technology* **2005**, *19*, 181.

(39) Tormoen, G. W.; Drelich, J.; Nalaskowski, J. *Journal of Adhesion Science and Technology* **2005**, *19*, 215.

(40) Briscoe, B. J.; Liu, K. K.; Williams, D. R. *Journal of Colloid and Interface Science* **1998**, *200*, 256.

(41) Tambe, N. S.; Bhushan, B. *Nanotechnology* **2004**, *15*, 1561.

(42) Haiat, G.; Barthel, E. *Langmuir* **2007**, *23*, 11643.

(43) Drelich, J.; Tormoen, G. W.; Beach, E. R. *Journal of Colloid and Interface Science* **2004**, *280*, 484.

(44) Savia, M.; Zhou, Q.; Ieee In *Ieee/Rsj 2010 International Conference on Intelligent Robots and Systems* 2010, p 5622.

(45) Tam, E.; Lhernould, M. S.; Lambert, P.; Delchambre, A.; Delplancke-Ogletree, M.-P. *Applied Surface Science* **2009**, *255*, 7898.

(46) Huang, Z.; Geyer, N.; Werner, P.; de Boor, J.; Goesele, U. *Advanced Materials* **2011**, *23*, 285.

(47) Bechelany, M.; Brioude, A.; Bernard, S.; Stadelmann, P.; Cornu, D.; Miele, P. *Crystengcomm* **2011**, *13*, 6526.

hal-00719432, version 1 - 19 Jul 2012

(48) Bernard, S.; Salles, V.; Li, J.; Brioude, A.; Bechelany, M.; Demirci, U. B.; Miele, P. *Journal of Materials Chemistry* **2011**, *21*, 8694.

(49) Bechelany, M.; Brioude, A.; Stadelmann, P.; Bernard, S.; Cornu, D.; Miele, P. *Journal of Physical Chemistry C* **2008**, *112*, 18325.

(50) Bechelany, M.; Brioude, A.; Bernard, S.; Cornu, D.; Miele, P. *Crystal Growth & Design* **2011**, *11*, 1891.

(51) Bechelany, M.; Brioude, A.; Bernard, S.; Ferro, G.; Cornu, D.; Miele, P. *Nanotechnology* **2007**, *18*, 335305.

hal-00719432, version 1 - 19 Jul 2012

TOC

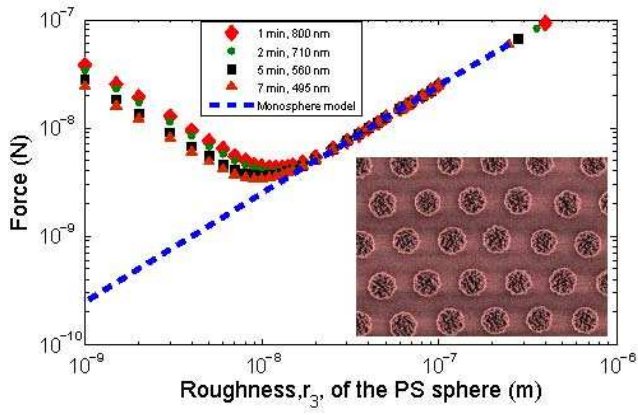

We report on the adhesion measurement on innovating structures such as non-closed packed PS spheres and organized Si NWs. The adhesion values of the pull-off force measured on these structures were very low (in the range of 2 to 30 nN), and suggest that these new nanostructures have non-adhesive properties.

hal-00719432, version 1 - 19 Jul 2012